

Received 10 April 2023, accepted 1 May 2023, date of publication 4 May 2023, date of current version 11 May 2023.

Digital Object Identifier 10.1109/ACCESS.2023.3272892

RESEARCH ARTICLE

On the Design of NOMA-Enhanced Backscatter Communication Systems

TUYEN T. HOANG¹, HOANG D. LE^{1,2}, (Member, IEEE), XUAN LUU NGUYEN¹, AND CHUYEN T. NGUYEN¹

¹School of Electrical and Electronic Engineering, Hanoi University of Science and Technology, Hanoi 100000, Vietnam

²School of Computer Science and Engineering, The University of Aizu, Aizuwakamatsu 965-8580, Japan


Corresponding author: Chuyen T. Nguyen (chuyen.nguyenthanh@hust.edu.vn)

ABSTRACT Non-orthogonal multiple access (NOMA) and backscatter communication (BackCom) are two emerging technologies for low-power Internet of Things (IoT) applications. This paper addresses the performance of a monostatic BackCom system employing the hybrid time-division multiple-access (TDMA)/power-domain (PD) NOMA, where a reader simultaneously serves multiple backscatter nodes (BNs). While the conventional schemes are mainly for static NOMA-aided monostatic BackCom systems, we instead introduce the design framework for dynamic systems. Moreover, we also present novel schemes to further improve the performance of such conventional static systems. Specifically, as for the static NOMA-enhanced monostatic BackCom systems, we investigate two schemes: (i) a *two-node pairing (TNP) scheme* to increase the possibility of successfully decoding NOMA groups by not randomly pairing BNs for such groups as in conventional approach and (ii) an *adaptive power reflection coefficient (APRC) scheme* to enhance the system performance by adjusting BN's power reflection coefficient based on the channel conditions. Regarding the dynamic NOMA-enhanced monostatic BackCom systems, two schemes, namely *dynamic-sized pairing (DSP)* and *hybrid APRC/DSP*, are proposed, in which the number of BNs in a NOMA group is not necessarily to be a fixed size. To illustrate the enhanced system using the proposed schemes, we analyze the performance of the BackCom system in terms of the number of successful backscatter nodes and the number of bits that can be successfully decoded by a controller/reader. The obtained results confirm the effectiveness of our proposed schemes compared to the conventional ones over the state-of-the-art.

INDEX TERMS Backscatter communications, non-orthogonal multiple access, user pairing scheme, adaptive power reflection coefficient scheme, dynamic-sized pairing scheme.

I. INTRODUCTION

Internet of Things (IoT) is an essential enabling application of the sixth-generation (6G) wireless networks [2]. Under the IoT paradigm, abundant sensors/small computing devices access the Internet and share their information [3]. Nevertheless, with the rapid development of IoT technology, massive connectivity, and power consumption are the major requirements for many IoT applications [4]. For the massive number of energy-constrained IoT devices, it is a great challenge to replace and/or recharge them frequently, especially in hazardous environments [5]. To this end, it is

The associate editor coordinating the review of this manuscript and approving it for publication was P. Venkata Krishna .

critical to investigate the technologies for future wireless networks with the abilities of large-scale access and extremely low power consumption. To this purpose, the combination of non-orthogonal multiple access (NOMA) and backscatter communication (BackCom) is expected to be one of the critical enabling technologies in the future 6G wireless network [6].

NOMA is a crucial technology to solve the critical issue of large-scale access by allowing multiple users to be served at the same time/frequency resources [7]. In general, there are two main NOMA schemes: power-domain (PD) NOMA and code-domain (CD) NOMA [8]. Compared to the CD-NOMA, the PD-NOMA, which exploits the difference in the channel gain among users for multiplexing, provides low latency

and high spectral efficiency [9]. In PD-NOMA, successive interference cancellation (SIC) is used by receivers to decode the received signals, which are from the superimposed code at the transmitters. Moreover, PD-NOMA has the capability to maintain user fairness on the same resource via judiciously tuning the transmitted power based on channel conditions. As a result, the PD-NOMA scheme has received much attention from both academia and industry [10].

On the other hand, the BackCom, which has recently grabbed tremendous attention from the research community, is a promising energy-harvesting technique for low-power IoT networks [11]. This technique realizes the information transmission by reflecting and modulating an incident radio frequency (RF) wave without power-hungry active components, e.g., oscillators, up-converters, and power amplifiers [12]. In general, there are three configurations in BackCom systems, namely monostatic, bistatic, and ambient backscatter configurations [13]. This paper focuses on the monostatic BackCom systems, e.g., for short-range radio frequency identification (RFID) applications. A monostatic BackCom system generally consists of two main components: a reader (or controller) and backscatter nodes (BNs). During the communication process, each BN tunes its antenna impedance and communicates with the reader by modulating and reflecting the incident RF signal via reflection coefficients. A portion of the incident RF signal power is harvested to supply the power for BN's circuit, while the remaining incident RF signal power is reflected back to the reader thanks to the reflection coefficients. It is noteworthy that the BackCom systems enable low-cost and low-power IoT applications compared to conventional energy-harvesting approaches [14], as reported in [13, Section II.A]. As a result, the BackCom systems can achieve information transmission via surrounding radio signals from ambient RF sources, without requiring a dedicated energy supply for BNs [15]. These energy-saving features make the BackCom become a prospective candidate for IoT applications in future wireless networks.

A. RELATED WORKS AND MOTIVATION

To exploit the unrivaled benefits of the above-mentioned technologies, the combination of NOMA and BackCom has recently attracted research efforts worldwide [16], [17], [18]. The NOMA-aided BackCom systems offer high spectral/energy efficiency and cost-effectiveness for collecting massive low-power IoT devices [19]. This makes such systems a candidate prime for green IoT networks [20]. Moreover, this integration is especially essential for the monostatic BackCom systems due to the following reason. In fact, a critical concern on the design of monostatic BackCom systems is the doubly near-far problem, where the modulated backscatter signals may suffer from a round-trip path loss [21]. In other words, if a BN is located far from the reader, it suffers from a higher energy outage probability as well as a lower modulated backscatter signal strength [13]. Nevertheless, this critical weakness, in turn, becomes an

advantage for such BackCom systems by integrating with PD-NOMA schemes. More specifically, the channel gain difference between near BN and far BN (compared to the reader) increases due to the doubly near-far problem, which can benefit from the PD-NOMA scheme. Therefore, it is necessary to exploit and investigate the performance of such NOMA-aided monostatic BackCom systems, where a proper design should be addressed.

1) RELATED WORKS

Driven by the potential and popularity of the integration of the PD-NOMA scheme and monostatic BackCom, several studies have recently addressed the design and performance evaluation for static NOMA-aided monostatic BackCom systems [22], [23], [24], [25], [26]. Particularly, Jing et al. provided the design guideline for the monostatic BackCom systems using a hybrid time-division multiple-access (TDMA)/PD-NOMA scheme, where the reflection coefficients for the multiplexed BNs from different NOMA groups are set to different values to utilize the PD-NOMA [22]. In [23], the authors introduced a mechanism to reduce the collisions in NOMA-aided BackCom systems, where a power level threshold for BNs was considered in the backscattering phase. The authors in [24] addressed the performance of NOMA-aided monostatic multi-antenna BackCom systems, in which a space division multiple access (SDMA) scheme was employed. In [25], the authors presented a transmitted power-driven channel access scheme, which controls the number of BNs contending the channel by tuning the transmitted power of the illuminator incrementally. Most recently, the authors optimized the average energy efficiency of NOMA-aided BackCom systems, where signals from two BNs were multiplexed on the frequency resource block using NOMA in each time slot [26].

It is noted that the computational complexity of employing the SIC technique in NOMA increases exponentially with a large number of backscatter nodes (BNs) [27]. To cope with this SIC issue as well as to exploit additional degrees of freedom, NOMA can be integrated with other orthogonal multiple access (OMA) schemes, e.g., space/time/frequency-division multiple access [28]. Such hybrid systems not only exploit different multiplexing domains to improve the system performance but also facilitate the practical implementation of NOMA in massive IoT [29]. Aside from [22] and [24], to the best of our knowledge, there are no other studies addressing the design of hybrid OMA/PD-NOMA for monostatic BackCom systems. More importantly, the design framework for dynamic NOMA-aided monostatic BackCom systems is still not available in the literature.

2) MOTIVATIONS

It is worth noting that the key idea in NOMA-aided BackCom systems is to utilize different backscattered power levels from different BNs, in which they are controlled to backscatter their data at the same time. From the above studies, the design

TABLE 1. A comparison of related works on NOMA-aided monostatic BackCom.

Ref.	Hybrid Scheme	BN Pairing	PRC	Dynamic
[22]	TDMA/NOMA	Random	Fixed	
[23]		Random	Fixed	
[24]	SDMA/NOMA	Random	Fixed	
[25]		Random	Fixed	
[26]		Random	Fixed	
[1]	TDMA/NOMA	TNP	Fixed	
Our study	TDMA/NOMA	TNP	APRC	✓

framework reported in [22] supports this idea. It provides criteria for choosing power reflection coefficients for which BNs are classified into different regions depending on their power levels. Nevertheless, there are three major drawbacks to this design framework. *Firstly*, the BNs are chosen from different regions for NOMA grouping in a random manner. This results in a high probability that the signal from the selected BN is not decoded successfully because of adverse issues on wireless channels. *Secondly*, the BNs are assigned by the constant power reflection coefficients (PRC) based on their locations, which is to make a significant difference in the channel gains. Using these fixed settings, nonetheless, may lead to poor performance over time-varying channel conditions. *Thirdly*, the design framework in [22] was for the static NOMA-aided BackCom systems only. In practical systems, BNs may enter and/or leave the reader’s coverage area frequently, in which dynamic schemes need to be addressed. From such limitations, it is necessary and important to provide novel schemes for the performance enhancement of conventional NOMA-aided monostatic BackCom systems, which motivates us to focus on this study.

B. MAJOR CONTRIBUTIONS AND ORGANIZATION

The primary objective of this paper is to offer novel schemes for the performance improvement of conventional NOMA-aided monostatic BackCom. Also, both static and dynamic monostatic BackCom are investigated. Here, it is worth noting that our initial report in [1] was the first to tackle one of the aforementioned limitations of the conventional approach, i.e., the disadvantage of random selection of BNs for NOMA groups. Particularly, a new user pairing scheme was proposed to improve the system performance in a static setting, where the weakest signal node from the near region is grouped with the weakest one from the far region. This study, nevertheless, considered the two-node NOMA scheme only and allocated the constant power reflection coefficients to BNs. Furthermore, the presented scheme in [1] is not applicable to the dynamic NOMA-aided BackCom systems. This paper, therefore, provides a comprehensive design framework for both static and dynamic NOMA-enhanced monostatic BackCom systems. We also boldly and explicitly contrast our study to the state-of-the-art in Table 1. In a nutshell, the initial work in [1] has been substantially extended as follows:

C₁: We present a design framework for static NOMA-enhanced BackCom systems, considering two-node

TABLE 2. Table of notations.

Symbol	Description
N	Total number of backscatter nodes (BNs)
M	NOMA group size
R	Outer radius of coverage area
R_1	Inner radius of coverage area
r	Distance between a BN and a reader
T	Time-slot duration
ξ_i	Power reflection coefficient of the i -th BN
P_i	Received power of the i -th BN
P_{Tx}	Reader’s transmitted power
α	Path-loss coefficient
L	Annular region
N_o	Noise Power
\bar{N}_S	Normalized number of successful BNs
\bar{N}_{near}	Average number of successful BNs in near subregion
\bar{N}_{far}	Average number of successful BNs in far subregion
N_{near}	Number of BNs in near subregion
N_{far}	Number of BNs in far subregion
p_n	Prob. of a BN being in the subregion specified by R_1 and r
p_f	Prob. of a BN being in the subregion specified by R and r

TABLE 3. Table of abbreviations.

Abbreviation	Description
APRC	Adaptive Power Reflection Coefficient
BackCom	Backscatter Communication
BN	Backscatter Node
CD	Code-Domain
DSP	Dynamic-Sized Pairing
IoT	Internet of Thing
NOMA	Non-Orthogonal Multiple Access
PD	Power-Domain
PRC	Power Reflection Coefficient
RF	Reader’s transmitted power
RFID	Radio Frequency Identification
SDMA	Space Division Multiple Access
SIC	Successive Interference Cancellation
SINR	Signal-to-Interference-plus-Noise Rate
TDMA	Time Division Multiple Access
TNP	Two Node Pairing

pairing (TNP) scheme [1] and novel adaptive power reflection coefficient (APRC) scheme.

Instead of randomly choosing BNs for NOMA groups as in [22], the TNP scheme selects NOMA groups based on the possibility of successful decoding. The TNP scheme is expected to predict and prevent unsuccessful transmissions from NOMA groups. In addition, the APRC scheme could increase the possibility of successful decoding in NOMA groups by adjusting BN’s power reflection coefficients depending on their channel conditions.

C₂: We introduce a design framework for dynamic NOMA-enhanced BackCom systems, considering the novel dynamic-sized pairing (DSP) and hybrid APRC/DSP schemes.

The conventional approach is applicable for static systems, in which the NOMA group size is fixed. To support dynamic systems, the DSP scheme is introduced, where its goal is to increase the number of successful NOMA groups in dynamic NOMA-enhanced BackCom systems. Moreover,

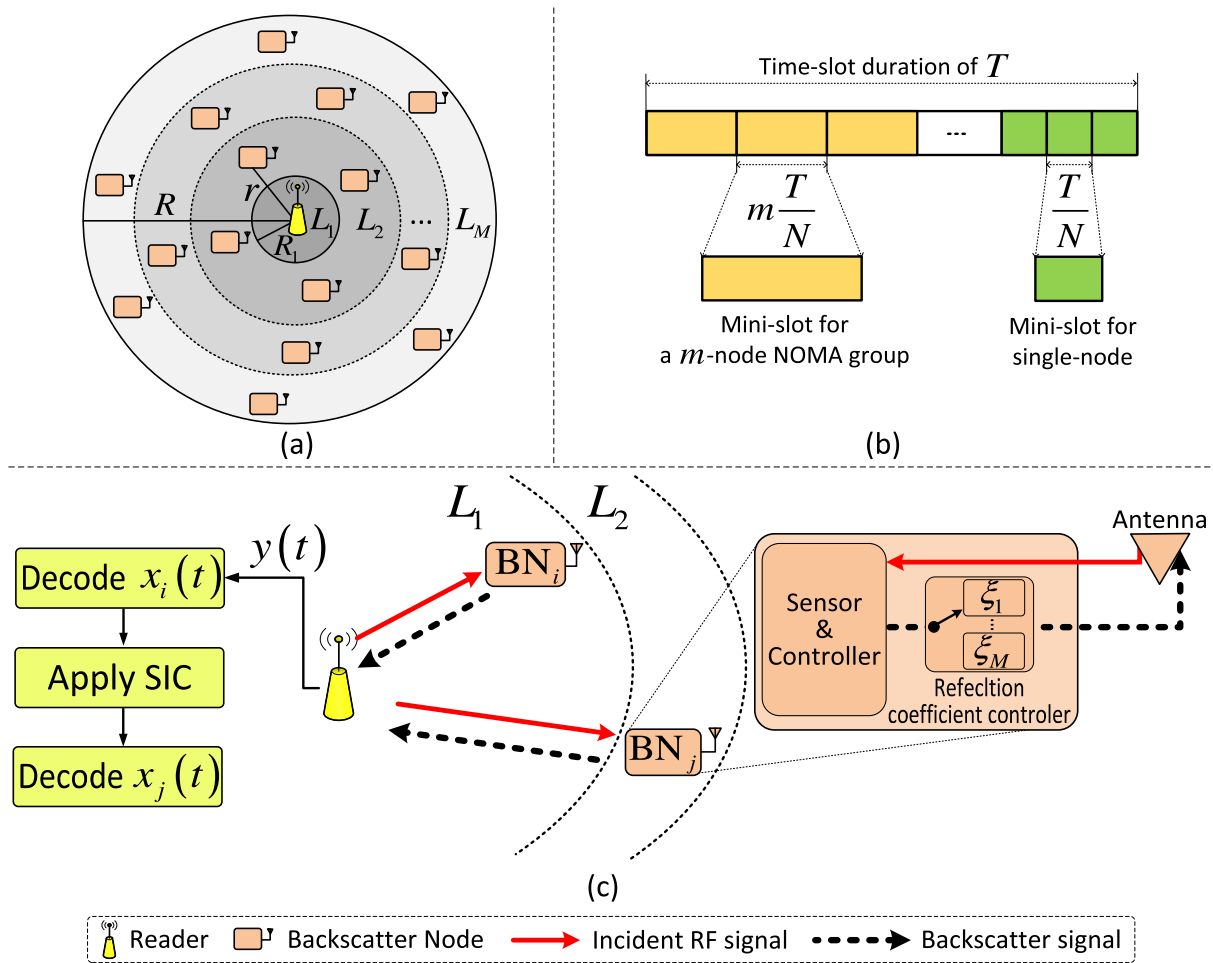


FIGURE 1. Illustration of (a) system model and (b) time-slot structure and (c) NOMA-aided BackCom system with $M = 2$.

we also present the hybrid APRC/DSP scheme, which combines the APRC and DSP schemes to further enhance the performance of dynamic NOMA-enhanced BackCom systems.

C_3 : We provide insightful results in terms of the number of successful backscatter nodes and the number of bits that can be successfully decoded by the reader to highlight the outperformance of our proposed schemes compared to the conventional ones.

The analysis of the TNP scheme regarding the number of successful backscatter nodes is provided. Monte Carlo simulations are also performed to validate the correctness of the theoretical analysis.

The rest of the paper is organized as follows. Section II describes the considered system model and conventional NOMA-aided BackCom systems. The proposed schemes for both static and dynamic NOMA-enhanced BackCom systems are presented in Section III, including TNP and APRC schemes for static systems as well as DSP and hybrid APRC/DSP schemes for dynamic systems. The simulation results are given in Section IV. Finally, we conclude the paper

in Section V. For the sake of explicit clarity, the definition of the variables used in our analysis as well as the description of the abbreviations in this paper are provided in Tables 2 and 3, respectively.

II. SYSTEM MODEL AND CONVENTIONAL APPROACH

A. SYSTEM DESCRIPTION

Our considered system, as shown in Fig. 1 (a), consists of a reader and N backscatter nodes (BNs), which can be sensors, IoT devices, and radio frequency identification (RFID) tags. In this study, the BNs are located randomly and independently around the reader, which is within an annular coverage area determined by an inner radius R_1 and an outer radius R [22], [30]. The purpose is to monitor a geographical area of radius of $[R_1, R]$, in which all ranges in the area are equally essential in terms of the sensing objective. As a result, the BNs are assumed to be uniformly distributed in the above interval. Then, the distance from a BN to the reader, denoted by r , can be modeled as the binomial point process, where its probability density function (PDF) is expressed as $f_r(r) = \frac{2r}{R^2 - R_1^2}$ [31].

The reader collects data from BNs using backscatter communications (BackCom). Particularly, the reader initially sends a request to specific BNs. Upon receiving the request, the BNs backscatter their data to the reader within the mini-slots of a time-slot duration.¹ Each time slot with a duration of T is partitioned into multiple mini-slots as depicted in Fig. 1 (b). A mini-slot accommodates the data from either a single BN or multiple BNs supported by the NOMA technique [32]. As a result, the time allocated to a mini-slot is defined as $m\frac{T}{N}$, where N is the total number of BNs, and m is the number of BNs multiplexed by the NOMA technique. Here, $m = 1$ for a single BN, while $2 \leq m \leq M$ for NOMA-aided multiple BNs with M the NOMA group size.

It is worth noting that systems using the power-domain NOMA technique require a considerable difference in the channel gains among users to decode data successfully [9]. To facilitate the NOMA-aided BackCom systems, each BN in a NOMA group is able to switch its power reflection coefficient of ξ in a range of values, i.e., $1 \geq \xi_1 \geq \xi_2, \dots, \geq \xi_M > 0$. This is controlled by the reader to make a significant difference in channel gains among the BNs. As a result, the received power at the reader from the i -th BN with the reflection coefficient of ξ_k can be expressed as

$$P_i = P_{Tx} \xi_k r_i^{-2\alpha}, \quad (1)$$

where $i \in \{1, 2, \dots, N\}$ and $k \in \{1, 2, \dots, M\}$. Additionally, P_{Tx} is the reader's transmitted power, and α is the path-loss coefficient.

B. CONVENTIONAL APPROACH

The conventional NOMA-aided monostatic BackCom system was reported in [22], where the hybrid TDMA/NOMA scheme was employed for uplink transmissions.

1) REVIEW OF CONVENTIONAL APPROACH

We now review the conventional approach reported in [22], which is summarized as follows.

Region Partition for NOMA Pairing: To facilitate the monostatic BackCom systems using the PD-NOMA scheme, the reader virtually divides its coverage area into M sub-regions, i.e., L_1, L_2, \dots, L_M , as depicted in Fig. 1 (a). Here, a sub-region L_m , with $m \in [1, M]$, is an annular region defined by the radii R_m and R_{m+1} ($R_m < R_{m+1}$ and $R_{M+1} = R$). Based on the training broadcast message along with a unique identity (ID) for each BN, the reader can obtain the channel state information (CSI), which is supposed to be reliable and up-to-date, and then classifies the BNs into different sub-regions. This depends on the signal power level of BNs received by the reader, which is estimated in (1). The reader randomly selects one BN per sub-region for NOMA grouping. It is worth noting that, if the M -size NOMA group is not feasible, the reader might repeat this process with $(M - 1)$ BNs, $(M - 2)$ BNs, and the rest.

¹In this paper, we focus on uplink communications, where the hybrid time-division multiple-access (TDMA)/power-domain non-orthogonal multiple access (NOMA) scheme is employed [8].

Time-Slot Structure and Power Reflection Coefficient: Similar to our considered monostatic BackCom system, the backscattering transmission of NOMA groups of multiple BNs as well as single BNs are taken within mini-slots in a time-slot duration as depicted in Fig. 1 (b). Different NOMA groups selected in a random manner by the reader are first transmitted in the mini-slot duration of $m\frac{2T}{N}$, while individual BNs respond later in the mini-slot time of $\frac{T}{N}$. On the other hand, the power reflection coefficient ξ is of importance of PD-NOMA-aided BackCom systems. This coefficient is to make the significant difference of channel gains to facilitate the NOMA pairing. The large values of the power reflection coefficient are assigned to BNs of near sub-region and vice versa. Here, the constant power reflection coefficient is assigned to each BN based on its location.

SIC-based NOMA Decoding: At the receiver side of the reader, the NOMA decoding is performed via the successive interference cancellation (SIC) technique, which is assumed to be perfect.² The decoding order is from the strongest signal to the weakest one. In other words, for each mini-slot of the NOMA group, the reader first detects and decodes the strongest signal, while treating the weaker ones as the interference. As transmission errors are unavoidable, the strongest signal can only be successfully decoded and extracted from the received signal if its signal-to-interference-and-noise ratio (SINR) satisfies a predefined threshold of γ_{th} . Assuming that the signal from i -th BN is the strongest one in a NOMA group size of M , where $i \in [1, M - 1]$. The condition for successfully decoding the i -th strongest signal, in which other signals from j -th BNs are treated as interference, can be expressed as

$$\text{SINR}_i = \frac{P_{Tx} \xi_i r_i^{-2\alpha}}{\left(\sum_{j=i+1}^M P_{Tx} \xi_j r_j^{-2\alpha} + N_o \right)} \geq \gamma_{th}, \quad (2)$$

where N_o is the noise power. If the condition in (2) is satisfied, the reader then decodes the second strongest signal and the rest. Otherwise, the strongest signal could not be decoded successfully, leading to the failed decoding of the remaining weaker ones.

2) EXAMPLE AND LIMITATIONS

The example and limitations regarding the conventional approach are described as follows.

Example: An example of the conventional NOMA-enhanced BackCom system is illustrated in Fig. 1 (c). Also, the NOMA group size is $M = 2$ corresponding to the two-BN pairing case. We assume that two BNs, i.e., BN_i and BN_j , forming a NOMA group belong to two different sub-regions, i.e., L_1 (near) and L_2 (far), respectively. Consider that BN_i and BN_j are paired using NOMA in a mini-slot of t . The

²In practice, the perfect SIC receiver is impossible due to the error propagation in the SIC decoding process [33]. For the sake of simplicity, this paper assumes the ideal SIC decoding at the receiver. Nevertheless, analyzing the performance of the proposed systems with imperfect SIC is beyond the scope of this work and can be further investigated in our future work.

received signal in the mini-slot t is, then, expressed as $y(t) = h_i x_i(t) + h_j x_j(t) + n(t)$, where h_i and h_j are the channel gains, while $x_i(t)$ and $x_j(t)$ are the reflected signals from BN_i and BN_j , respectively. Additionally, $n(t)$ is the Gaussian noise. Assuming that the BN_i experiences a better channel gain than that of the BN_j , i.e., $h_i > h_j$. Thus, the reader first decodes the signal of BN_i , i.e., $x_i(t)$, removes the signal by SIC, and then decodes the signal of BN_j , i.e., $x_j(t)$.

Limitations: There are three critical limitations of the conventional approach, as follows:

- *Firstly*, it is the random selection of BNs for NOMA groups. This might lead to a high probability of unsuccessful decoding and significant deterioration of the system's performance.
- *Secondly*, the constant power reflection coefficients are used for BNs. This may result in poor performance over the time-varying channel conditions between the reader and BNs.
- *Thirdly*, the conventional approach is applicable to static NOMA-aided BackCom systems. Nevertheless, many practical BackCom applications are dynamic, in which BNs may enter and/or leave the reader's coverage area frequently. This results in the variation of BN population and requires a different approach.

III. PROPOSED NOMA-ENHANCED BackCom SYSTEMS

From the critical restrictions of the conventional approach mentioned in Section II, this section presents the proposed NOMA-enhanced BackCom Systems. Notably, the improvement schemes for static NOMA-enhanced BackCom Systems, including two-node pairing (TNP) as well as adaptive power reflection coefficient (APRC) schemes, are first introduced. Then, the pairing schemes for dynamic NOMA-enhanced BackCom Systems, i.e., dynamic-sized pairing (DSP) and APRC-assisted DSP schemes, are presented.

A. NOMA-ENHANCED BackCom: STATIC SYSTEMS

1) TWO-NODE PAIRING (TNP) SCHEME

This scheme is to address the first drawback of the conventional approach described in Section II. Notably, instead of randomly selecting BNs for NOMA groups from different sub-regions, the TNP scheme chooses NOMA groups based on the possibility of successfully decoding. It is expected to predict and prevent unsuccessful transmissions/decoding from NOMA groups. More specifically, following the training phase reported in [22], the reader categorizes N BNs into near and far sub-regions.³ Correspondingly, $N/2$ BNs with higher backscattered power levels, i.e., $P_1 \geq P_2 \geq \dots \geq P_{N/2}$, belong to the near sub-region, in which its power reflection coefficient is set to ξ_1 . At the same time, the rest of ones with $P_{N/2+1} \geq P_{N/2+2} \geq \dots \geq P_N$ are in the

³Here, we mainly focus on the two-node pairing NOMA groups with $M = 2$, which is widely considered in the literature. It is, however, straightforward to extend for the general M case, i.e., the so-called M -node pairing scheme.

Algorithm 1 Reader Operation for TNP Scheme

```

/* INITIATION: */
1 for node in network do
2   | node sets the power reflection coefficient  $\xi_1$ 
3 end
4 ;
/* COLLECTING: */
5 Collect signal level of  $N$  nodes;
/* SPLITTING AND SET UP: */
6 Sort  $N$  nodes by signal power level;
7 Split nodes from 1 to  $N/2$  into Near_subregion;
8 Split nodes from  $N/2 + 1$  to  $N$  into Far_subregion;
9 for node in Near_subregion do
10  | node sets the power reflection coefficient  $\xi_1$ ;
11 end
12 for node in Far_subregion do
13  | node sets the power reflection coefficient  $\xi_2$ ;
14 end
/* USER PAIRING SCHEME: */
15 while Near_subregion not empty do
16  |  $i \leftarrow \text{Near\_subregion.back}()$ ;
17  |  $j \leftarrow \text{Near\_subregion.back}()$ ;
18  Calculate  $\text{SINR}_i$ ;
19  if  $\text{SINR}_i \geq \gamma$  then
20    Pair nodes  $i, j$  to a NOMA group;
21    Far_subregion.pop_back();
22    Near_subregion.pop_back();
23  else
24    Set node  $i$  to transmit in a single time slot;
25    Near_subregion.pop_back();
26  end
27 end
28 while Far_subregion not empty do
29  |  $k \leftarrow \text{Far\_ubregion.pop\_back}()$ ;
30  Set  $k$  to transmit in a single time slot;
31 end
/* TRANSMIT: */
32 Send request NOMA groups and single nodes (if have) to transmit
    sequentially.

```

far sub-region, where its power reflection coefficient is set to ξ_2 . Here, the power reflection coefficients ξ_1 and ξ_2 , with $\xi_1 > \xi_2$, are constant values.⁴

It is worth noting that the terms *near* and *far* represent the groups of BNs with higher and lower signal powers, respectively. The reader pairs the BNs from the near sub-region and far sub-region, i.e., one BN from the near group and another BN from the far group. Particularly, the BN with the lowest power level from the near sub-region (i.e., $P_{N/2}$) is paired with the one having the lowest power level from the far sub-region (i.e., P_N). Then, for each pair of BNs, the reader pre-estimates the SINR as in (2) to examine the pairing possibility, i.e.,

- If the $\text{SINR} \geq \gamma_{\text{th}}$: a NOMA group is created for the transmission.
- If the $\text{SINR} < \gamma_{\text{th}}$: the BN in the near sub-region is not selected for NOMA pairing to avoid a high probability of unsuccessful decoding. This BN is, then, controlled to transmit in the mini-slots for single-node as depicted in Fig. 1(b). Another BN belonging to the near sub-region

⁴Unlike conventional PD-NOMA systems, actively updating the transmit power is not possible for passive BNs in BackCom ones. Instead, the power reflection coefficients are used to facilitate the NOMA pairing, in which a larger coefficient is set to the near sub-region and vice versa. To guarantee the fairness of BNs in the SIC decoding, the selection of these coefficients is provided in [22, Section III].

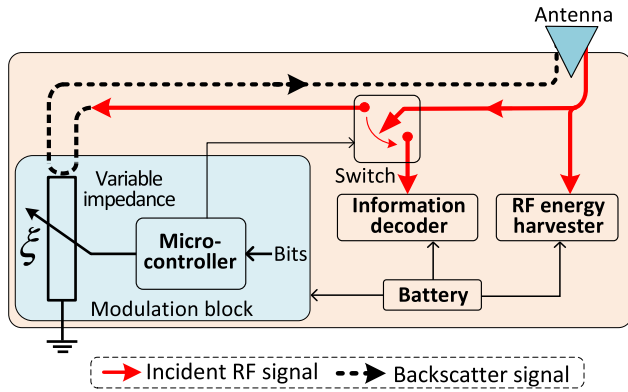


FIGURE 2. The structure of backscatter node with variable power reflection coefficients.

with a stronger power level (i.e., P_{N-1}) compared to the previous one is chosen to pair with the selected BN in the far sub-region.

This pairing process is performed until all BNs are considered. Finally, the reader requests NOMA groups and single BNs to transmit in the time slot containing multiple mini-slots as illustrated in Fig. 1(b).

In summary, the pseudo-code, which describes the reader operation of the TNP scheme, is provided in Algorithm 1. In addition, the analysis of the number of successful BN transmissions is provided in Appendix A.

2) ADAPTIVE POWER REFLECTION COEFFICIENT (APRC) SCHEME

This scheme aims to address the second disadvantage of the conventional approach mentioned in Section II. In particular, a feasible solution to tackle the poor performance issue of the conventional NOMA-aided BackCom systems over the time-varying channel conditions is the adaptive power reflection coefficient (APRC) scheme. For the APRC scheme, instead of using constant power reflection coefficients, i.e., $\xi_i = \text{constant}$, for BNs, the reader can adjust these coefficients depending on the channel conditions between the reader and BNs. This, in turn, could increase the possibility of successful decoding in NOMA groups over the time-varying channel conditions.

To do so, we consider the condition for successfully decoding the i -th BN from the NOMA groups with other j -th BNs, as shown in (2). In other words, the SINR of the i -th BN satisfies a predefined threshold of γ_{th} , i.e., $\text{SINR}_i \geq \gamma_{\text{th}}$. Then, the power reflection coefficient of ξ_i can be adjusted so that the i -th BN is decoded successfully, i.e.,

$$\xi_i \geq \frac{\gamma_{\text{th}} \left(\sum_{j=i+1}^M P_j + N_o \right)}{P_{\text{Tx}} r_i^{-2\alpha}} = \xi_i^{\text{opt}}, \quad (3)$$

where γ_{th} is the predefined threshold for successful decoding, while P_j is determined in (1). The power reflection coefficients for BNs are adjusted adaptively as follows:

Algorithm 2 Reader Operation for APRC Scheme

```

/* INITIATION: */
1 for i = 1 to N do
2   BNi.ξ = ξmax; // BNs set their power
   reflection coefficient
/* COLLECTING: */
3 Collect signal level from N nodes;
/* SPLITTING AND SET UP: */
4 Sort N nodes by signal power level;
5 K = N/M; // number of BNs in each
   sub-region
6 for i = 1 to N do
7   Ri ← {};
8   for j = 1 to N do
9     if (i - 1) × K < j & j ≥ i × K then
10      Ri.add(BNj);
11    end
12  end
13 end
/* USER PAIRING SCHEME: */
14 m = 1; // number of NOMA groups
15 while K > 0 do
16   Gm ← {}; // NOMA group
17   for i = 1 to N do
18     Gm.add(Ri.popRandom());
19   end
20   K = K - 1;
21   m = m + 1;
22 end
/* ADJUST ADAPTIVE POWER REFLECTION
   COEFFICIENT: */
23 for i = 1 to m do
24   for n = 1 to Gi.size() do
25     Gi[n].ξ = min(ξmax, ξnopt);
26   end
27 end
/* TRANSMIT: */
28 for i = 1 to m do
29   Send request NOMA groups Gi transmit data;
30 end
31 end
    
```

- The power reflection coefficient for the i -th BN, i.e., ξ_i , is controlled in a range from ξ_i^{opt} to ξ_{max} with $\xi_{\text{max}} \leq 1$.
- The coefficient ξ_i should be adjusted as the minimal value, i.e., $\xi_i = \min \left\{ \xi_i^{\text{opt}}, \xi_{\text{max}} \right\}$, in order to (i) *guarantee its successful decoding* and (ii) *reduce the interference to other BNs in the NOMA group*.

It is worth noting that the APRC scheme uses the random selection for NOMA group pairing as the conventional approach to reduce the system complexity. In addition, the structure of BNs implementing the APRC scheme is illustrated in Fig. 2. The BN is a passive node that harvests energy from an incident RF signal transmitted by the reader. The signal reflection is due to an intentional mismatch between the antenna and load impedance. By varying the load impedance, the power reflection coefficient of the i -th BN, i.e., ξ_i , can be adjusted. Besides, interested readers can refer to [34, Section 2] for more details of this structure.

In summary, the pseudo-code of reader operation for the APRC scheme is presented in Algorithm 2.

B. NOMA-ENHANCED BackCom: DYNAMIC SYSTEMS

1) DYNAMIC-SIZED PAIRING (DSP) SCHEME

The conventional approach is applicable for static NOMA-aided BackCom systems, where the NOMA group size is

Algorithm 3 Reader Operation for DSP Scheme

```

1  /* INITIATION: */
2  for i = 1 to N do
3    BNi.ξ = ξmax; // BNs set their power
4    reflection coefficient
5  /* COLLECTING: */
6  Collect signal level of N nodes;
7  /* SPLITTING AND SET UP: */
8  Sort N nodes by signal power level;
9  Set BNs B = {BN1, BN2, ..., BNN};
10 /* USER PAIRING SCHEME: */
11 m = 1; // number of NOMA groups
12 while B.size() > 0 do
13   Gm ← {}; // NOMA group
14   B.top().ξ = ξM;
15   Gm.add(B.pop());
16   for i = M - 1 to 1 do
17     Pithreshold = γ (∑n=i+1M Pn + N0);
18     for j = B.size() to 1 do
19       ξB[j] = ξi;
20       if Pj ≥ Pithreshold then
21         Gm.add(BNj);
22         B.remove(BNj);
23         break;
24       end
25     end
26   end
27   m = m + 1;
28 end
29 /* TRANSMIT: */
30 for i = 1 to m do
31   Send request NOMA groups Gi transmit data;
32 end

```

fixed. This may not (i) be suitable for dynamic systems, in which the number of BNs is varied accordingly to time, and (ii) be efficient due to the fixed size of the NOMA group. To tackle these issues, the dynamic-sized pairing (DSP) scheme is presented, in which its goal is to increase the number of successful NOMA groups while supporting dynamic systems. The major differences between the DSP scheme and the conventional approach are threefold:

- *Firstly*, the DSP scheme does not virtually divide the reader's coverage into regions, which is based on the power levels of BNs.
- *Secondly*, it is the dynamic NOMA group size, in which the number of BNs in a NOMA group is not necessarily to be M .
- *Thirdly*, the selection of BNs for NOMA groups is not random, which is similar to the TNP scheme.

In particular, the reader performs the training phase to collect information of BNs, such as the number of nodes, IDs, and backscatter powers. Also, the reflection coefficients of BNs are set to be the maximum value of ξ_{\max} . Assuming that there are K BNs at time instant t in our considered system, in which K could be varied according to time. These BNs are, then, sorted by the reader accordingly to their power levels, i.e., $P_1 \geq P_2 \geq P_3 \geq \dots \geq P_K$. For NOMA grouping, the maximum NOMA group size is determined by M_{\max} , in which the number of BNs in each group is equal to or smaller than M_{\max} . For BN pairing in each NOMA group, the reader chooses the BN with the lowest power level (e.g., P_K) to pair with BNs with higher power levels (e.g., P_{K-1})

that satisfy the condition for successful NOMA decoding as in (2). This process is performed until reaching the maximum NOMA group size, e.g., $M_{\max} = 5$ and BNs with power levels $P_K, P_{K-1}, \dots, P_{K-5}$.

Here, if the number of BNs selected for a NOMA group reaches the maximal value defined by the maximum NOMA group size of M_{\max} , the grouping process is continued with the remaining BNs to create another NOMA group. Otherwise, the NOMA group size is not necessarily to be M_{\max} , whose size is equal to the number of selected BNs if this number does not reach M_{\max} . This process is performed until all BNs are considered. Then, the reader requests both NOMA groups and single BNs to transmit during a time slot that consists of multiple mini-slots, as depicted in Fig. 1(b).

In summary, the pseudo-code of reader operation for the DSP scheme is described in Algorithm 3.

2) HYBRID APRC/DSP SCHEME

The power reflection coefficients of BNs in the DSP scheme are, nevertheless, constant values. To further enhance the performance of dynamic NOMA-aided BackCom systems, the hybrid APRC/DSP scheme is introduced, which is the combination of APRC and DSP schemes. In other words, the reader can adjust the power reflection coefficients of BNs in dynamic systems using the DSP scheme. More specifically, instead of using the maximum power reflection coefficient for all BNs as in the DSP scheme, i.e., $\xi_i = \xi_{\max}$, these coefficients are varied accordingly to the channel conditions between the reader and BNs. Also, the value of ξ_i should be chosen as the minimum value, i.e., $\xi_i = \min \{ \xi_i^{\text{opt}}, \xi_{\max} \}$.

IV. SIMULATION RESULTS AND DISCUSSIONS

This section presents the performance evaluation for the proposed NOMA-enhanced monostatic BackCom, both static and dynamic systems. We also comparatively discuss the performance of our proposed system with (i) conventional BackCom with TDMA (without NOMA scheme) and (ii) conventional NOMA-aided monostatic BackCom reported in [22]. Monte Carlo simulations are performed with 10000 runs. The parameters used for the simulations, unless otherwise noted, are as follows: The inner and outer radius of coverage zones: $R_1 = 20$ m and $R = 100$ m. The total number of BNs is $N = 60$. The number of NOMA groups is set to 2. The reflection coefficients $\xi_1 = 0.7$, $\xi_2 = 0.5$, $\xi_3 = 0.3$, $\xi_4 = 0.1$, $\xi_5 = 0.05$ and $\xi_{\max} = 1$. The path-loss coefficient $\alpha = 2.5$, the reader's transmitted power $P_{\text{Tx}} = 25$ dBm, the noise power $N_0 = -90$ dBm. The time-slot duration is set to be 1 second, and each BN sends 60 bits during a mini-slot [22].

A. PERFORMANCE COMPARISON

Firstly, we highlight the effectiveness of our proposed schemes for static NOMA-enhanced BackCom systems, including the two-node pairing (TNP) and adaptive power reflection coefficient (APRC) schemes, in comparison with

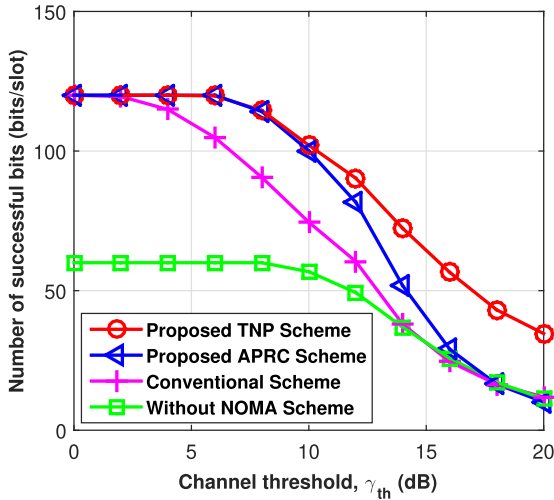


FIGURE 3. Average number of successfully decoded bits versus channel thresholds for different schemes in static BackCom systems.

(i) the conventional BackCom with TDMA (without NOMA scheme) and (ii) the conventional BackCom using the hybrid TDMA/NOMA scheme [22]. Here, as for the conventional BackCom systems with TDMA, only one BN is scheduled to modulate and then backscatter its signal to the reader in each mini-slot.

Particularly, Fig. 3 investigates the number of successful bits transmitted per time slot for each BN of different schemes. Also, different channel thresholds, i.e., γ_{th} , are taken into account. As is evident, the BackCom systems using the hybrid NOMA/TDMA schemes retain a better performance than BackCom systems using TDMA schemes. This is because the duration of each mini-slot under NOMA is m times larger than that with TDMA only. Furthermore, when comparing the performance of the BackCom systems using the hybrid NOMA/TDMA, as expected, our proposed schemes, i.e., the TNP and APRC schemes, outperform the conventional one reported in [22] over a range of channel thresholds. Additionally, the TNP scheme can achieve the highest performance in comparison with the APRC and conventional schemes.

This fact is further highlighted in Fig. 4, where the proposed TNP and APRC schemes outperform the conventional NOMA-aided BackCom in terms of the normalized number of successful BNs. The reason is that these schemes could increase the possibility of successful decoding in NOMA groups by pairing selected BNs, which is not in a random manner (the TNP scheme), or adjusting the power reflection coefficients depending on the channel conditions (the APRC scheme). When comparing the TNP scheme with the APRC scheme, it is observed that the TNP scheme can achieve a better performance than that of the APRC scheme. However, the complexity of the TNP scheme increases when the NOMA group size increase, while the APRC scheme offers a simpler solution for large values of NOMA group size. As a result, it is recommended to use the TNP scheme and the APRC

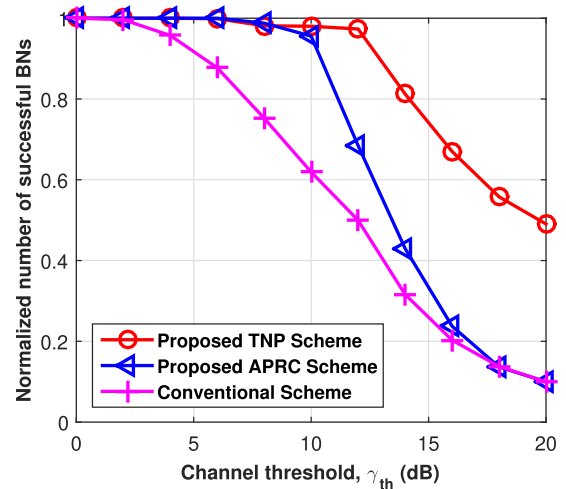


FIGURE 4. Normalized number of successful BNs versus channel thresholds for different schemes in static BackCom systems.

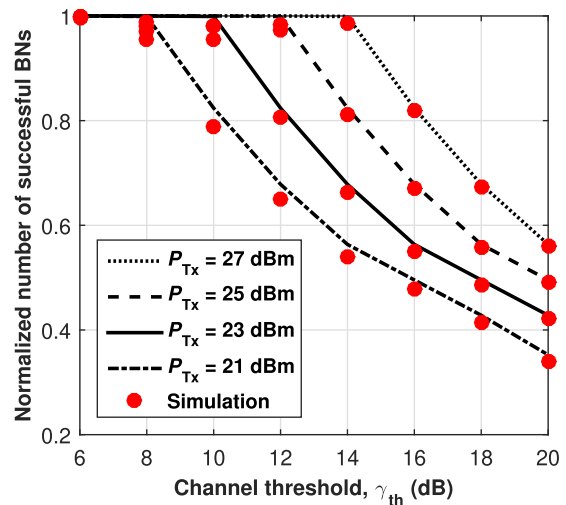


FIGURE 5. Normalized successful BNs versus channel threshold for the static systems using the TNP scheme.

scheme for small ($M = 2$) and large values ($M > 2$) of NOMA group size, respectively. For example, when $\gamma_{th} = 12$ dB, the normalized number of successful BNs are 0.98, 0.68, and 0.5 for the TNP, APRC, and conventional schemes, respectively.

B. NUMBER OF SUCCESSFUL BACKSCATTER NODES

Next, We investigate the performance of the proposed NOMA-enhanced monostatic BackCom, both static and dynamic systems, in terms of the normalized number of successful BNs. It is defined as the average number of successful BNs over the total number of BNs.

Figure 5 analyzes the normalized number of successful BNs versus the channel thresholds for the static NOMA-enhance BackCom systems using the TNP scheme. Also, different values of reader's transmitted powers, i.e., $P_{Tx} = 21$ dBm, 23 dBm, 25 dBm, 27 dBm, are taken into

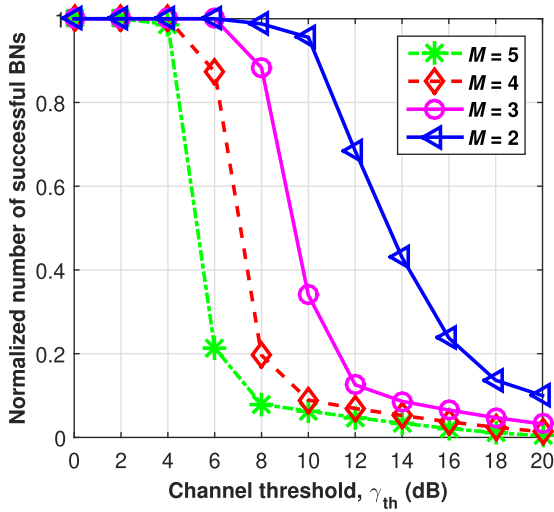


FIGURE 6. Normalized successful BNs versus channel threshold for the static systems using the APRC scheme.

account. As is evident, larger channel thresholds require higher levels of transmitted power to achieve the best performance. In other words, using this figure, we can decide the minimum power levels corresponding to the channel thresholds to retain the maximum value of the normalized number of successful BNs. For example, the minimum power levels are chosen to be $P_{Tx} = 21$ dBm, 23 dBm, 25 dBm, and 27 dBm for respectively the given channel thresholds of γ_{th} of 8 dB, 10 dB, 12 dB, 14 dB, to maintain the highest value of the normalized number of successful BNs. Indeed, the selection of such minimal power levels plays an essential role in energy-efficient NOMA-aided BackCom systems. Also, in this figure, the simulation results match perfectly with the analytical ones, as expected. This confirms the model’s correctness and analysis of the TNP scheme.

The performance of the APRC scheme in terms of the normalized number of successful BNs is illustrated in Fig. 6. Also, different values of the NOMA group size, i.e., $M = 2, 3, 4, 5$, are taken into account. As is evident, when the NOMA group size increases, the normalized number of successful BNs decreases. The reason is that a larger NOMA group size reduces the possibility of successful decoding in NOMA systems. For example, when the channel threshold of $\gamma_{th} = 10$ dB, the normalized number of successful BNs for the APRC scheme are 0.1, 0.15, 0.38, and 0.95 for the NOMA group size of $M = 5, 4, 3, 2$, and 1, respectively.

In Fig. 7, we investigate the performance of dynamic NOMA-enhanced BackCom systems using the DSP scheme. Also, different reader’s transmitter powers, i.e., $P_{Tx} = 21$ dBm, 23 dBm, 25 dBm, 27 dBm, are considered. As seen, the higher values of the normalized number of successful BNs require higher levels of transmitted power. For instance, to maintain the normalized number of successful BNs of 0.8, the transmitted power levels required are 21 dBm, 23 dBm, 25 dBm, and 27 dB, for the channel thresholds γ_{th} of 12 dB, 14 dB, 16 dB, and 18 dB, respectively.

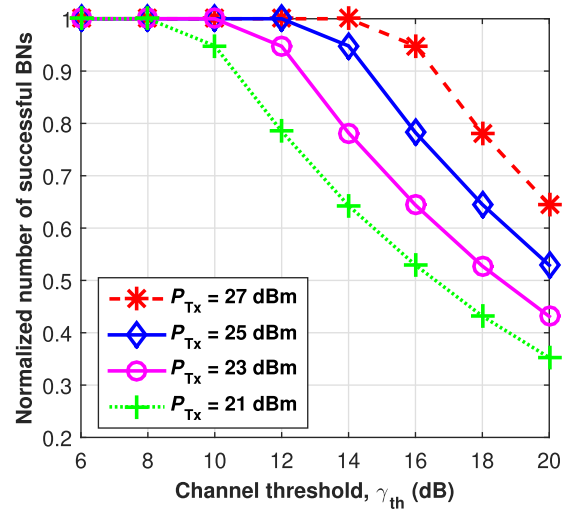


FIGURE 7. Normalized successful BNs versus channel threshold for the dynamic systems using the DSP scheme.

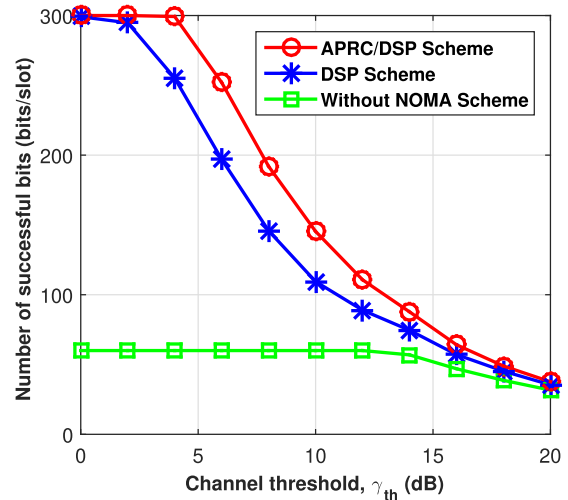


FIGURE 8. Number of successful bits versus channel threshold for DSP and hybrid APRC/DSP schemes in dynamic systems.

C. NUMBER OF SUCCESSFULLY TRANSMITTED BITS

Finally, we evaluate the performance of dynamic NOMA-enhanced monostatic BackCom systems regarding the number of successfully decoded bits. We also compare our proposed schemes with the benchmark of dynamic BackCom systems with TDMA (without NOMA). Here, due to the constraint on the computational complexity and delay, we assume the maximum NOMA group size is $M_{max} = 5$.

In particular, we investigate the performance of dynamic NOMA-enhanced BackCom systems in terms of the average number of successfully transmitted bits in Figs. 8 and 9. Both the DSP scheme and the hybrid APRC/DSP scheme are considered. Figure 8 illustrates the system performance over a range of channel thresholds, given $P_{Tx} = 25$ dBm. As seen from this figure, the number of successfully decoded bits decreases with increasing the channel thresholds γ_{th} , where the performance of the dynamic NOMA-aided

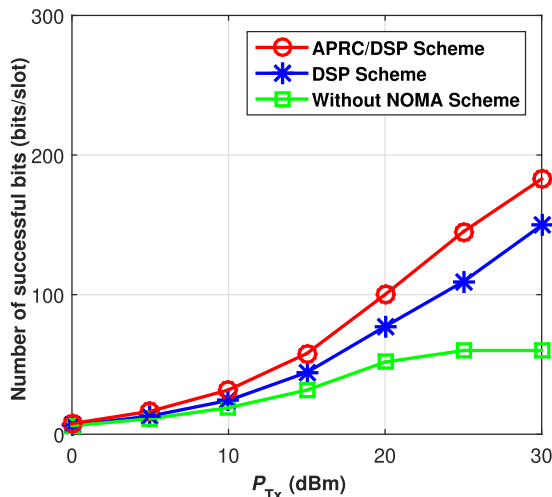


FIGURE 9. Number of successful bits versus transmitted power for DSP and hybrid APRC/DSP schemes in dynamic systems.

BackCom system is degraded. This is because the higher channel thresholds of γ_{th} , the lower probability of successful decoding in the NOMA group. On the other hand, as seen, the hybrid APRC/DSP scheme achieves better performance than the DSP scheme for different channel thresholds. The reason is that the hybrid APRC/DSP scheme not only takes advantage of the DSP scheme but also can adjust the power reflection coefficients of the APRC scheme to increase the possibility of successful decoding in NOMA groups.

The same observation is illustrated in Fig. 9 varying in different transmitted powers, where $\gamma_{th} = 10$ dB. Using this figure, we can decide the power levels to maintain a target performance level. For instance, to retain the number of successfully transmitted bits of above 100 bits/slot, the required transmitted power levels for the DSP and hybrid APRC/DSP schemes are 25 dBm and 20 dBm, respectively. From Figs. 8 and 9, it is clear that our proposed schemes outperform the conventional BackCom systems using the TDMA only.

V. CONCLUSION

This paper presented the design frameworks for both static and dynamic NOMA-enhanced monostatic BackCom systems. Specifically, we first introduced the novel schemes, i.e., TNP and APRC, to further enhance the performance of conventional static NOMA-aided monostatic BackCom systems. The TNP scheme was expected to predict and prevent unsuccessful transmissions from NOMA groups, while the APRC could increase the possibility of successful decoding in NOMA groups. Then, we addressed the design of dynamic NOMA-enhanced monostatic BackCom systems, in which two new schemes, i.e., DSP and hybrid APRC/DSP, were presented to support such dynamic systems. The DSP scheme allowed the dynamic NOMA group size, while the hybrid APRC/DSP scheme used the APRC approach to further enhance the performance of the DSP scheme. The performance metrics, including the number of

successful backscatter nodes and the number of bits that can be successfully decoded by the reader, were investigated. The simulation results supported the proper selection of our proposed schemes compared to the conventional ones. Moreover, through the obtained results, we suggest using respectively the TNP and the APRC schemes for small ($M = 2$) and large ($M > 2$) values of NOMA group size. We also showed that the hybrid APRC/DSP scheme maintains better performance than the DSP scheme in dynamic NOMA-enhanced monostatic BackCom systems. Monte Carlo simulations were performed to validate the correctness of the theoretical analysis for the TNP scheme. Future work will investigate the analytical framework for the considered NOMA-enhanced BackCom systems using the above-proposed schemes in case of imperfect SIC. Also, the performance optimization of the proposed NOMA-enhanced BackCom systems will be considered.

APPENDIX A

PERFORMANCE ANALYSIS OF THE TNP SCHEME

The number of successfully decoded BNs is the primary performance metric investigated in this study. Here, we focus on the performance analysis of the TNP scheme, in which the NOMA group size is set to $M = 2$. Let \bar{N}_S be the normalized number of successful BNs. It is defined by the ratio of the number of successful BNs and the total number of BNs, which can be expressed as

$$\bar{N}_S = \frac{\bar{N}_{near} + \bar{N}_{far}}{N}, \tag{4}$$

where \bar{N}_{near} and \bar{N}_{far} are respectively the average number of successful BNs in near and far regions, which are written as

$$\begin{cases} \bar{N}_{near} &= P_{near} \left(r \leq \left(\frac{\gamma N}{P_{Tx} \xi_1} \right)^{-\frac{1}{2\alpha}} \right) \mathcal{N}_{near}, \\ \bar{N}_{far} &= P_{far} \left(r \leq \left(\frac{\gamma N}{P_{Tx} \xi_2} \right)^{-\frac{1}{2\alpha}} \right) \mathcal{N}_{far}, \end{cases} \tag{5}$$

where $\mathcal{N}_{near} = \mathcal{N}_{far} = N/2$ are the total number of BNs in near and far regions. In addition, $P_{near}(r)$ and $P_{far}(r)$ are the probabilities that a node of distance r belongs to the near and far sub-regions, respectively. Here, it is noted that, after sorting N nodes based on the measured signal levels, $N/2$ nodes, i.e., $1, 2, \dots, N/2$, having stronger signal power levels belong to the near sub-region while the rest of the nodes are in the far one. The probability that a node at a distance r is the i -th node in the sorted list is, then, expressed as

$$p_{i,r} = C_{N-1}^{N-i} p_n(r)^{i-1} p_f(r)^{N-i} f_r(r), \tag{6}$$

where $C_{N-1}^{N-i} \triangleq \frac{(N-1)!}{(N-i)!(i-1)!}$ and $f_r(r) = \frac{2r}{R^2 - R_1^2}$ defined in Section II. Additionally, $p_n(r)$ and $p_f(r)$ are respectively the probabilities that a BN is at a region specified by (R_1, r) and

$$P_{\text{near}}\left(r \leq \left(\frac{\gamma N}{P_{\text{Tx}}\xi_1}\right)^{-\frac{1}{2\alpha}}\right) = 2 \int_{R_1}^{\left(\frac{\gamma N}{P_{\text{Tx}}\xi_1}\right)^{-\frac{1}{2\alpha}}} \frac{2r}{(R^2 - R_1^2)^N} \sum_{j=0}^{\frac{N}{2}-1} C_{N-1}^j \times (r^2 - R_1^2)^j (R^2 - r^2)^{N-1-j} dr, \quad (9)$$

$$P_{\text{far}}\left(r \leq \left(\frac{\gamma N}{P_{\text{Tx}}\xi_2}\right)^{-\frac{1}{2\alpha}}\right) = 2 \int_{R_1}^{\left(\frac{\gamma N}{P_{\text{Tx}}\xi_2}\right)^{-\frac{1}{2\alpha}}} \frac{2r}{(R^2 - R_1^2)^N} \sum_{j=0}^{\frac{N}{2}-1} C_{N-1}^j \times (r^2 - R_1^2)^{N-1-j} (R^2 - r^2)^j dr, \quad (10)$$

(r, R), which can be calculated by

$$\begin{aligned} p_n(r) &= \int_{R_1}^r f_x(x) dx = \int_{R_1}^r \frac{2x}{R^2 - R_1^2} dx = \frac{r^2 - R_1^2}{R^2 - R_1^2}, \\ p_f(r) &= \int_r^R f_x(x) dx = \int_r^R \frac{2x}{R^2 - R_1^2} dx = \frac{R^2 - r^2}{R^2 - R_1^2}. \end{aligned} \quad (7)$$

Using (6), the probabilities, i.e., $P_{\text{near}}(r)$ and $P_{\text{far}}(r)$, are determined as

$$\begin{cases} P_{\text{near}}(r) = \sum_{i=1}^{\frac{N}{2}} p_{i,r}, \\ P_{\text{far}}(r) = \sum_{i=\frac{N}{2}+1}^N p_{i,r}. \end{cases} \quad (8)$$

To complete (4), we need to determine the probabilities of a successful BN belonging to near or far sub-regions in (5). Based on (8), these probabilities are written as (9) and (10), shown at the top of the page, where $j = N - i$. After some mathematical manipulations, the average number of successful BNs in (5) can be computed as

$$\begin{aligned} \bar{N}_{\text{near}} &= N \sum_{j=0}^{\frac{N}{2}-1} C_{N-1}^j \frac{\left(\left(\frac{\gamma N_o}{P_{\text{Tx}}\xi_1}\right)^{-\frac{1}{2\alpha}} - R_1^2\right)^{j+1}}{j+1} \\ &\times {}_2F_1\left(j+1, j+1-N; j+2; \frac{\left(\frac{\gamma N_o}{P_{\text{Tx}}\xi_1}\right)^{-\frac{1}{2\alpha}} - R_1^2}{R^2 - R_1^2}\right), \end{aligned} \quad (11)$$

$$\begin{aligned} \bar{N}_{\text{far}} &= N \sum_{j=0}^{\frac{N}{2}-1} C_{N-1}^j \frac{\left(\left(\frac{\gamma N_o}{P_{\text{Tx}}\xi_2}\right)^{-\frac{1}{2\alpha}} - R_1^2\right)^{N-j}}{N-j} \\ &\times {}_2F_1\left(N-j, -j; N+1-j; \frac{\left(\frac{\gamma N_o}{P_{\text{Tx}}\xi_2}\right)^{-\frac{1}{2\alpha}} - R_1^2}{R^2 - R_1^2}\right). \end{aligned} \quad (12)$$

By substituting (11) and (12) into (4), we can obtain the normalized number of successful BN \bar{N}_S .

ACKNOWLEDGMENT

An earlier version of this paper was presented in part at the 2020 IEEE Eighth International Conference on Communications and Electronics (ICCE) [1].

REFERENCES

- [1] L. X. Nguyen, C. T. Nguyen, V. X. Phan, and A. T. Pham, "A novel user pairing scheme for non-orthogonal multiple access backscatter communication," in *Proc. IEEE 8th Int. Conf. Commun. Electron. (ICCE)*, Jan. 2021, pp. 509–514.
- [2] E. Sisinni, A. Saifullah, S. Han, U. Jennehag, and M. Gidlund, "Industrial Internet of Things: Challenges, opportunities, and directions," *IEEE Trans. Ind. Informat.*, vol. 14, no. 11, pp. 4724–4734, Nov. 2018.
- [3] A. Al-Fuqaha, M. Guizani, M. Mohammadi, M. Aledhari, and M. Ayyash, "Internet of Things: A survey on enabling technologies, protocols, and applications," *IEEE Commun. Surveys Tuts.*, vol. 17, no. 4, pp. 2347–2376, 4th Quart., 2015.
- [4] L. Da Xu, W. He, and S. Li, "Internet of Things in industries: A survey," *IEEE Trans. Ind. Informat.*, vol. 10, no. 4, pp. 2233–2243, Nov. 2014.
- [5] L. Zhang, Y.-C. Liang, and M. Xiao, "Spectrum sharing for Internet of Things: A survey," *IEEE Wireless Commun.*, vol. 26, no. 3, pp. 132–139, Jun. 2019.
- [6] W. U. Khan, A. Ihsan, T. N. Nguyen, Z. Ali, and M. A. Javed, "NOMA-enabled backscatter communications for green transportation in automotive-Industry 5.0," *IEEE Trans. Ind. Informat.*, vol. 18, no. 11, pp. 7862–7874, Nov. 2022.
- [7] M. Vaezi, G. A. A. Baduge, Y. Liu, A. Arafa, F. Fang, and Z. Ding, "Interplay between noma and other emerging technologies: A survey," *IEEE Trans. Cognit. Commun. Netw.*, vol. 5, no. 4, pp. 900–919, Dec. 2019.
- [8] X. Wei, H. Al-Obiedollah, K. Cumanan, Z. Ding, and O. A. Dobre, "Energy efficiency maximization for hybrid TDMA-NOMA system with opportunistic time assignment," *IEEE Trans. Veh. Technol.*, vol. 71, no. 8, pp. 8561–8573, Aug. 2022.
- [9] T. Park, G. Lee, W. Saad, and M. Bennis, "Sum rate and reliability analysis for power-domain nonorthogonal multiple access (PD-NOMA)," *IEEE Internet Things J.*, vol. 8, no. 12, pp. 10160–10169, Jun. 2021.
- [10] O. Maraqa, A. S. Rajasekaran, S. Al-Ahmadi, H. Yanikomeroğlu, and S. M. Sait, "A survey of rate-optimal power domain NOMA with enabling technologies of future wireless networks," *IEEE Commun. Surveys Tuts.*, vol. 22, no. 4, pp. 2192–2235, 4th Quart., 2020.
- [11] C. Xu, L. Yang, and P. Zhang, "Practical backscatter communication systems for battery-free Internet of Things: A tutorial and survey of recent research," *IEEE Signal Process. Mag.*, vol. 35, no. 5, pp. 16–27, Sep. 2018.
- [12] A. W. Nazar, S. A. Hassan, H. Jung, A. Mahmood, and M. Gidlund, "BER analysis of a backscatter communication system with non-orthogonal multiple access," *IEEE Trans. Green Commun. Netw.*, vol. 5, no. 2, pp. 574–586, Jun. 2021.
- [13] N. Van Huynh, D. T. Hoang, X. Lu, D. Niyato, P. Wang, and D. I. Kim, "Ambient backscatter communications: A contemporary survey," *IEEE Commun. Surveys Tuts.*, vol. 20, no. 4, pp. 2889–2922, 4th Quart., 2018.
- [14] X. Lu, P. Wang, D. Niyato, D. I. Kim, and Z. Han, "Wireless networks with RF energy harvesting: A contemporary survey," *IEEE Commun. Surveys Tuts.*, vol. 17, no. 2, pp. 757–789, 2nd Quart., 2015.
- [15] K. Han and K. Huang, "Wirelessly powered backscatter communication networks: Modeling, coverage, and capacity," *IEEE Trans. Wireless Commun.*, vol. 16, no. 4, pp. 2548–2561, Apr. 2017.
- [16] Q. Zhang, L. Zhang, Y.-C. Liang, and P. Y. Kam, "Backscatter-NOMA: An integrated system of cellular and Internet-of-Things networks," in *Proc. IEEE Int. Conf. Commun. (ICC)*, May 2019, pp. 1–6.

- [17] A. Farajzadeh, O. Ercetin, and H. Yanikomeroglu, "UAV data collection over NOMA backscatter networks: UAV altitude and trajectory optimization," in *Proc. IEEE Int. Conf. Commun. (ICC)*, May 2019, pp. 1–7.
- [18] G. Yang, X. Xu, and Y.-C. Liang, "Resource allocation in NOMA-enhanced backscatter communication networks for wireless powered IoT," *IEEE Wireless Commun. Lett.*, vol. 9, no. 1, pp. 117–120, Jan. 2020.
- [19] J. Wang, H.-T. Ye, X. Kang, S. Sun, and Y.-C. Liang, "Cognitive backscatter NOMA networks with multi-slot energy causality," *IEEE Commun. Lett.*, vol. 24, no. 12, pp. 2854–2858, Dec. 2020.
- [20] X. Li, H. Liu, G. Li, Y. Liu, M. Zeng, and Z. Ding, "Effective capacity analysis of AmBC-NOMA communication systems," *IEEE Trans. Veh. Technol.*, vol. 71, no. 10, pp. 11257–11261, Oct. 2022.
- [21] J. Guo, X. Zhou, S. Durrani, and H. Yanikomeroglu, "Backscatter communications with NOMA (invited paper)," in *Proc. 15th Int. Symp. Wireless Commun. Syst. (ISWCS)*, Aug. 2018, pp. 1–5.
- [22] J. Guo, X. Zhou, S. Durrani, and H. Yanikomeroglu, "Design of non-orthogonal multiple access enhanced backscatter communication," *IEEE Trans. Wireless Commun.*, vol. 17, no. 10, pp. 6837–6852, Oct. 2018.
- [23] J. Guo, S. Durrani, and X. Zhou, "Monostatic backscatter system with multi-tag to reader communication," *IEEE Trans. Veh. Technol.*, vol. 68, no. 10, pp. 10320–10324, Oct. 2019.
- [24] G. Sacarello and Y. H. Kim, "Beamforming and reflection coefficient control for multi-antenna backscatter communication with nonorthogonal multiple access," *IEEE Access*, vol. 9, pp. 56104–56114, 2021.
- [25] R. Valentini, P. Di Marco, and F. Santucci, "A NOMA scheme for IoT enabled by selective powering of passive backscattering nodes," *IEEE Commun. Lett.*, vol. 26, no. 9, pp. 2195–2199, Sep. 2022.
- [26] F. D. Ardakani, R. Huang, and V. W. S. Wong, "Joint device pairing, reflection coefficients, and power control for NOMA backscatter systems," *IEEE Trans. Veh. Technol.*, vol. 71, no. 4, pp. 4396–4411, Apr. 2022.
- [27] Y. Liu, Z. Qin, M. ElKashlan, Z. Ding, A. Nallanathan, and L. Hanzo, "Nonorthogonal multiple access for 5G and beyond," *Proc. IEEE*, vol. 105, no. 12, pp. 2347–2381, Dec. 2017.
- [28] M. Zeng, A. Yadav, O. Dobre, and H. V. Poor, "Energy-efficient joint user-RB association and power allocation for uplink hybrid NOMA-OMA," *IEEE Internet Things J.*, vol. 6, no. 3, pp. 5119–5131, Feb. 2019.
- [29] X. Wei, H. Al-Obiedollah, K. Cumanan, W. Wang, Z. Ding, and O. A. Dobre, "Spectral-energy efficiency trade-off based design for hybrid TDMA-NOMA system," *IEEE Trans. Veh. Technol.*, vol. 71, no. 3, pp. 3377–3382, Mar. 2022.
- [30] A. Bletsas, S. Sialchalou, and J. N. Sahalos, "Anti-collision backscatter sensor networks," *IEEE Trans. Wireless Commun.*, vol. 8, no. 10, pp. 5018–5029, Oct. 2009.
- [31] Z. Khalid and S. Durrani, "Distance distributions in regular polygons," *IEEE Trans. Veh. Technol.*, vol. 62, no. 5, pp. 2363–2368, Jun. 2013.
- [32] S. Zeb, Q. Abbas, S. A. Hassan, A. Mahmood, R. Mumtaz, S. M. H. Zaidi, S. A. R. Zaidi, and M. Gidlund, "NOMA enhanced backscatter communication for green IoT networks," in *Proc. 16th Int. Symp. Wireless Commun. Syst. (ISWCS)*, Aug. 2019, pp. 640–644.
- [33] W. U. Khan, X. Li, M. Zeng, and O. A. Dobre, "Backscatter-enabled NOMA for future 6G systems: A new optimization framework under imperfect SIC," *IEEE Commun. Lett.*, vol. 25, no. 5, pp. 1669–1672, May 2021.
- [34] W. Liu, K. Huang, X. Zhou, and S. Durrani, "Next generation backscatter communication: Systems, techniques, and applications," *EURASIP J. Wireless Commun. Netw.*, vol. 2019, no. 1, pp. 1–11, Mar. 2019.



HOANG D. LE (Member, IEEE) received the B.E. degree in electronics and communications from the Hanoi University of Science and Technology (HUST), Vietnam, in 2016, and the M.E. and Ph.D. degrees in computer science and engineering from The University of Aizu (UoA), Japan, in 2018 and 2021, respectively. He was a Postdoctoral Researcher with the Computer Communications Laboratory, UoA, from 2021 to 2023. He is currently an Associate Professor with the School of Computer Science and Engineering, UoA. His current research interests include cross-layer design for optical wireless networks, hybrid FSO/RF for satellite/UAV communications, quantum cryptography, and machine learning. He is a member of ACM. He was a recipient of several honors/awards, including the 2018 KICS/IEEE ICTC Best Paper Award, the 2019 IEEE VTS Tokyo Chapter Young Researcher Encouragement Award, the 2019 IEEE ComSoc Sendai Chapter Student Excellent Research Award, and the 2022 IEEE ICCE Best Paper Award. He is the Young Researcher to participate in the 9th Heidelberg Laureate Forum 2022.



XUAN LUU NGUYEN received the B.E. and M.E. degrees in electronics and communications from the Hanoi University of Science and Technology (HUST), Vietnam, in 2020 and 2022, respectively. His research interest includes protocol design for BackCom systems.



CHUYEN T. NGUYEN received the B.E. degree in electronics and telecommunications from the Hanoi University of Science and Technology (HUST), Vietnam, in 2006, the M.S. degree in communications engineering from National Tsing Hua University, Taiwan, in 2008, and the Ph.D. degree in informatics from Kyoto University, Japan, in 2013. From September 2014 to November 2014, he was a Visiting Researcher with The University of Aizu, Japan. He is currently an Associate Professor with the School of Electrical and Electronic Engineering, HUST. His current research interests include communications theory and applications, with a particular emphasis on protocol design for the Industrial Internet of Things applications and wireless/optical networks. He received the Fellow Award from the Hitachi Global Foundation, in August 2016, the First Best Paper Award from the 2019 IEEE ICT, and the Best Paper Award from the 2018 KICS/IEEE ICTC and the 2019 IEEE ICC.



TUYEN T. HOANG received the B.S. and M.S. degrees in telecommunications from the Hanoi University of Science and Technology (HUST), Vietnam, in 2012 and 2015, respectively, where he is currently pursuing the Ph.D. degree with the School of Electrical and Electronic Engineering. His research interest includes protocol design for RFID-based systems.